Indian Journal of Geo-Marine Sciences
Vol. 42(8), December 2013, pp. 1006-1012

A study on the swimming pattern of legged underwater robot

[1]Daehyun Kim & [2]Jihong Lee
Department of Mechatronics Engineering, Chung-Nam National University
79 Daehag-ro 99, Yuseong-gu, Daejeon 305-764, KOREA
[E-mail : [1] kdhenjoy@cnu.ac.kr, [2] jihong@cnu.ac.kr]

Received 5 December 2012; revised 22 October 2013

KIOST (Korea Institute of Ocean Science and Technology) in Korea has been developing an underwater robot, Crabster. This robot has been designed to be able to walk and swim with legs without screws. However, it is difficult to get fluid dynamics of joint-robots in the water. Therefore, we conducted simulations with an optimization algorithm for swimming by considering simplified fluid dynamics in this paper. Drag-coefficient to be applied to the simulation war approximated values calculated by CFD (Computational Fluid Dynamics: Tecplot 360, ANSYS). In addition, Optimized swimming patterns were applied to a real robot. As a result, we estimated drag coefficient by comparing drag force from simulation with optimized algorithm with drag force from the experiment with a real robot. And we will verify the swimming pattern from the optimized algorithm for swimming is most efficient through the experiment.

[**Keywords:** Underwater Robot, Optimal swimming pattern, CFD (Computational Fluid Dynamics), Biomimetics]

Introduction

Amid flourishing high-tech these days, Biomimetics robot is no longer the new technology. As for a Magazine Article, see[1], based on idea of secretion from natural substance and living things, it's been increasingly applied to medical and military sectors at the moment when modern technology reached its limitations. Particularly the study on Boimimetics robot has been accelerated in the area of land, sea and air. Research of the bird or flying insect has been often adopted for study on Boimimetics robot. Flying principle was explained based on analysis of flapping by the bird or insect for a Journal Article, see[2] and microminiaturized flying object was fabricated in a way of imitating the flapping of the fly or insect using piezo actuator for a Journal Article, see[3].

When it comes to Biomimetics land-robot, more robots were tested than air-robot. Particularly as for a Military robot workshop, see[4], a snake-shaped robot which crawls or rolls is able to explore in the limited space and still work while it's overturned. For a Proceedings Paper, see[5] shows the walking robot equipped with various sensors which produce the data making it sustain stable walking.

Recently, development of underwater robot has actively been in progress in the world as ROV(Remotely Operator Vehicle) and AUV(Autonomous Unmmanded Vehicle) style for a Conference paper, see[6-8]. But despite of the increasingly important submarine resources, the other robots than ROV or AUV which are capable of exploring and sampling the submarine resources have yet to be developed.

KIOST, beginning in 2010, launched the R&D project to develop the robot, dubbed CRABSTER (CRAB + (LOB) STER) as shown in Figure 1 in a bid to enhance the safety and efficiency of resource exploration. This robot was designed to cope with the tidal current and limited visibility and propeller-free design enabled it to generate less floating natters. In this study, optimal swimming pattern was selected for simulation and applied to actual robot so as to compare the simulation with test data for verification. Optimal structure of the robot was determined as a result of observing the swimming patterns of the underwater creatures for a University Technical Report, see[9] and a conference paper, see[10].

Fig. 1— CRABSTER under development

Materials and Methods

Design and Manufacture of a robot-leg

Kinematic design of creature's leg

Kinematic design of triaxial robot's a leg and simulation were carried out using swimming pattern as shown in Figure 2.

Third link was the joint allows the area can be adjusted depending on angle. D-H parameter is by the table number. eg:Table1.

In this paper, the length of Link 1 is designed a_1=287 mm, the length of link 3 is d_1=210 mm in the text by the table number. eg: Table 1. As link 2 is shorter, it used the coordinate of joint 3 shown in Figure 3.

The robot shown in Figure 3 was designed considering some important standpoints.

1. The structure for waterproofing.
2. Water tank design to prevent water tightness effect.

Results and Discussion

Manufacture of robot

Consequently, the robot manufactured is shown in Figure 4 time and cost for waterproofing design could be reduced by arranging the motor above the water surface.

As seen in (b) of Figure 4, the cover of water tank was placed 10 cm away from joint 1 to prevent water overflow and sloshing so as to reduce the water effect, which then could not verified because of difficulty in modeling the water effect.

Simulation for optimizing swimming pattern considering hydrodynamics

In this chapter, drag coefficient which is one of the important elements to the movement of underwater robot was obtained using computational fluid program and was applied to optimal swimming pattern simulation.

Simulation for estimating drag coefficient of the manufactured robot

The sectional area of link 1 and 3 is as (a) of Figure 4 link 1 can do X-Y in plane motion and in roll-joint-shape link 3, sectional area varies depending on angle. Drag coefficient depending on angle of roll-joint was calculated through simulation as Figure 5. Simulation in Figure 5 shows the estimated fluid coefficient at every 30 degrees. Since the program measuring the drag coefficient on real-time base considering the movement of the object has yet to be developed, flow

Table 1 — D-H parameter

	θ_i	α_i	d_i	a_i
1	θ_1	90	L_1	0
2	θ_2	0	0	L_2
3	θ_3	0	0	L_3

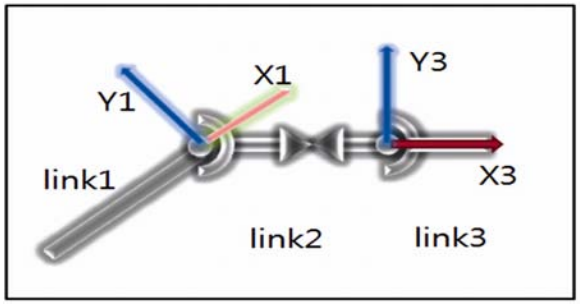

Fig. 2 — Kinematic design of a robot-leg

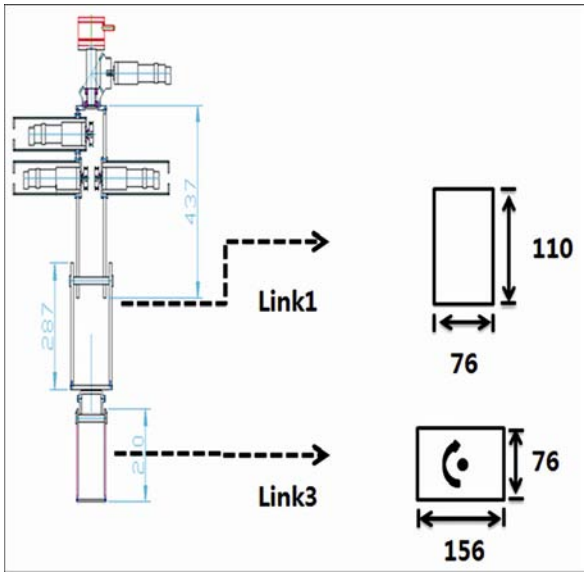

Fig. 3 — Robot-leg drawing and link section (a) Robot leg manufactured (b) Robot leg and water tank

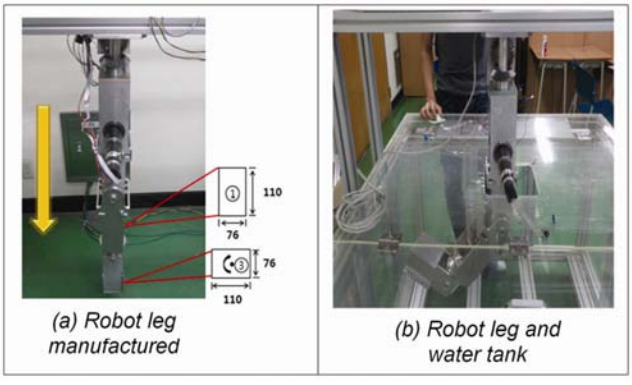

Fig. 4 — Robot drawing and link section

analysis is carried out at specific angle or motion and thus the method indicated in Figure 5 was adopted in this study. In each angle of Figure 5, the first figure shows the flow and the second figure shows the estimated drag coefficient. Drag coefficient at 120 degree and 150 degree have minus value. Because the fluid flowing from the right to the left at 30 degree in Figure 5. Corresponds to 150 degree and likewise, 60 degree equals 120 degree and thus it's calculated by simply changing the flow direction of the fluid.

According to the estimate of drag coefficient is some cases through the simulation, the result was referred in the text by the table number.eg: Table 2. Generally, drag was once thought to be greater at

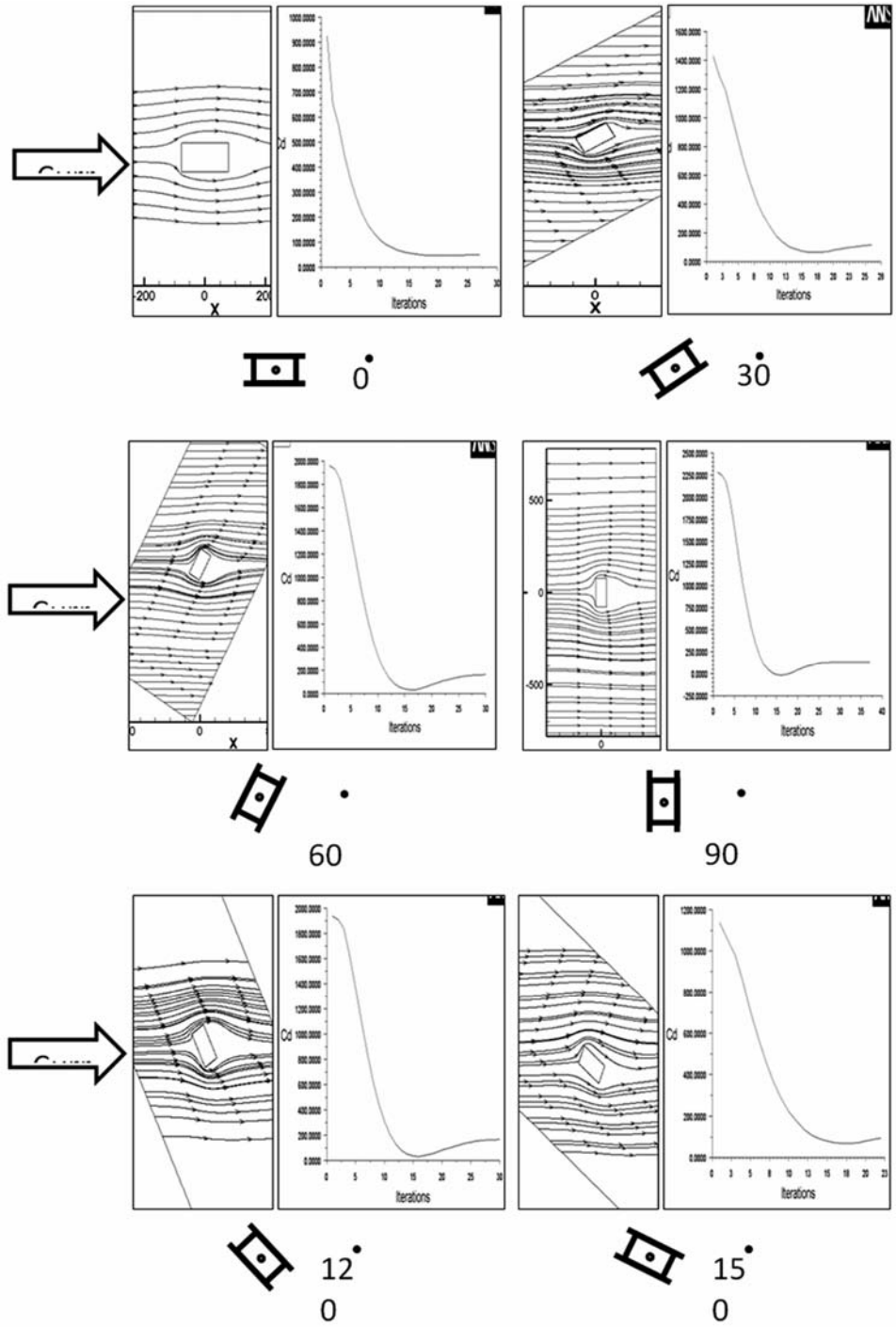

Fig. 5 — Simulation for estimating drag coefficient using

90 degree, but viewing the following cases, fluid resistance was rather more severe at 60 degree and 120 degree. The coefficient was estimated to produce the maximum force in propelling direction by applying the estimated value to optimized algorithm.

The figures calculated in Table 2 do not indicate the drag coefficient at every angle and thus, it's approximated with the function using polynomial explanation as seen in Equation (1) σ_j refers to the angle of robot leg toward the flow and when applying this to $C_{Dj}(\sigma_j)d_{pj}$ in Equation (2), drag coefficient (df_{Dj}) could be estimated. This can be expressed with the graph as seen in Figure 6.

$$C_{Dj}(\sigma_j) = A\sigma_j^6 + B\sigma_j^5 + C\sigma_j^4 + D\sigma_j^3 + E\sigma_j^2 + F\sigma_j + G \quad \dots (1)$$

$$df_{Dj} = -\frac{1}{2}\rho C_{Dj}(\sigma_j) d_{pj} \| {}^i\vec{v}^{ni} \| {}^i v^{ni} dl \quad \dots (2)$$

Swimming pattern optimization simulating using estimated drag coefficient

Dynamics for simulation is as Equation (3) Dynamics of underwater robot has drag elements in addition to common joint robot.

$$M(\theta)\ddot{\theta} + C(\theta,\dot{\theta}) + D(\theta,\dot{\theta}) + G(\theta) = \tau \quad \dots (3)$$

Where, $M(\theta)$ is $n \times n$ inertia matrix of robot leg and $C(\theta,\dot{\theta})$ is $n \times 1$ vector o centrifugal force and coriolis.

Table 2 — Estimate of drag coefficient

	Drag coefficients	Fluid speed(m/s)
0°	0.5001	1
30°	1.1707	1
60°	1.6355	1
90°	1.3108	1
120°	1.6925	1
150°	1.1607	1

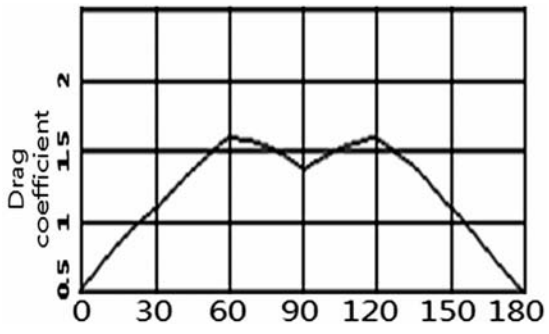

Fig. 6 — Drag coefficient graph approximated using Equation (1) (a) Swimming pattern when drag coefficient varies (-78.579N) (b) Swimming pattern when drag coefficient does not vary (-58.228N)

$G(\theta)$ is $n \times 1$ gravity vector and $D(\theta,\dot{\theta})$ is the equation for fluid drag. Generally, fluid drag is the sum of Drag and Lift. Drag term is expressed as Equation (4) while lift term is expressed as Equation (5). Accordingly, $D(\theta,\dot{\theta})$ is expressed as Equation (6).

$$\tau_{Di} = \sum_{j=1}^{n} \tau_{Dij}, i = 1,2,\cdots,n \quad \dots (4)$$

$$M = \begin{bmatrix} M_{11} & 0 & 0 \\ 0 & M_{22} & M_{23} \\ 0 & M_{32} & M_{33} \end{bmatrix} \quad \dots (5)$$

$$M_{11} = (\frac{1}{3}m_2 + m_3)L_2^2 c_2^2 + \frac{1}{2}m_3 L_3^2 c_{23}^2 + m_3 L_2 L_3 c_2 c_{23} \quad \dots (6)$$

$$M_{22} = -\frac{1}{6}m_2 L_2^2 c_1^2 c_2^2 s_2 + \frac{1}{2}m_2 L_2^2 c_1^2 c_2^2 s_2 + \frac{1}{3}m_2 L_2^2 s_1^2 s_2^2 + \frac{1}{3}m_2 L_2^2 c_2^2$$

$$M_{23} = -\frac{1}{6}m_3 L_3^2 c_1^2 s_{23} c_{23} + \frac{1}{6}m_3 L_3^2 s_1^2 s_{23}^2 - \frac{1}{6}m_2 L_3^2 c_{23}^2 + \frac{1}{2}m_2 L_2^3 + \frac{1}{2}m_3 L_2 L_3 c_3 M_{32} = M_{23} \quad \dots (7)$$

When describing above equation in drag force, it's as Equation (8) which is used as object function of optimization algorithm.

$$f = \int_0^T e_d^T \cdot JM^{-1}Ddt \quad \dots (8)$$

e_d^T is unit direction vector, J is jacobian Matrix, M^{-1} is inverse matrix and D is related to fluid drag. The value of this equation is produced in torque and the unit is Nm. In above object function, it's set as $e_d^T = [100]$ so as to produce the maximum force in positive direction of X. the value of coefficient at maximum force is considered to be the optimal swimming pattern. Initial constraints of the simulation is as. Eg: Table 3.

Table 3 — Constraints

	Angle(Degree)			Velocity(rad/s)			Accel(rad/s^2)		
Joint	1	2	3	1	2	3	1	2	3
Max	90	30	30	+1.05	+1.05	+1.05	+1.05	+1.57	+1.57
Min	-90	-60	-90	-1.05	-1.05	-1.05	-1.05	-1.57	-1.57

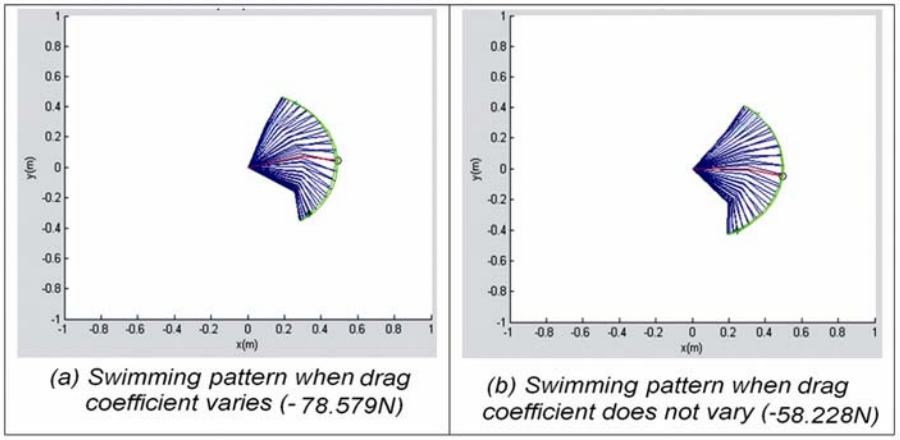

Fig. 7 — Result of swimming pattern optimization simulation, (a) Sensor measuring in air (b)Sensor measuring in water

As the robot designed above performs 2D motion only shile sectional area of the last link varies, it's compared with the 2D simulation result (-0.253N) in Figure 7.

Figure 7 shows the comparison between (a) when sectional area of the robot was varied depending on angle of link 3 and (b) when sectional area was not varied. In conclusion, (a) was greater by about 40%. That is, swimming while varying the sectional area appeared to be more efficient.

Test by applying swimming pattern to real robot

In this chapter, the test to estimate the drag by applying each joint route of optimal swimming pattern obtained from the simulation was conducted. The test to measure the buoyancy was first conducted to eliminate the buoyancy elements working on robot and then drag was measured depending on joint speed and comparison between the drag and other swimming patterns than optimal pattern when applying the optimal swimming pattern, thereby verifying the swimming pattern obtained from simulation was the optimal one Figure 8.

Buoyancy measuring test

In Equation (8), G is the item considering buoyancy. G in the air equals to Equation (9). But G in the water is as Equation (10):

$$M(\vec{q})\vec{q} + C(\vec{q},\vec{q}) + D(\vec{q},\vec{q}) + G(q) = \tau \quad \ldots (10)$$

$$g = \sum_{j=i}^{n} - m_j g U_{ji}^{j} \bar{r}_j, i = 1,2,\cdots,n$$

m 10

$$g = \sum_{j=i}^{n} - ((m_j + \rho\nabla_i)g + \rho\nabla_i)U_{ji}^{j} \bar{r}_j, i = 1,2,\cdots,n \quad \ldots (11)$$

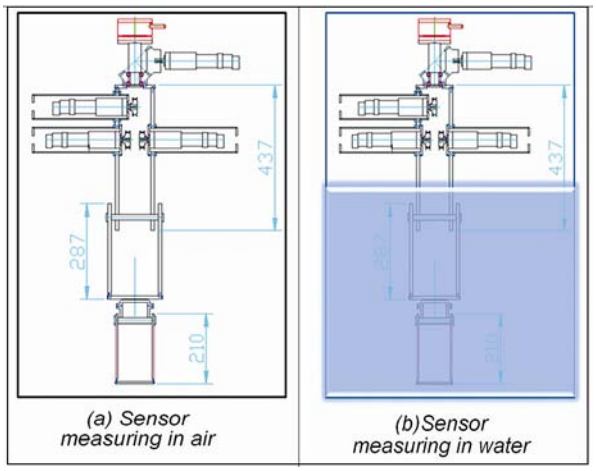

Fig. 8 — Buoyancy measuring

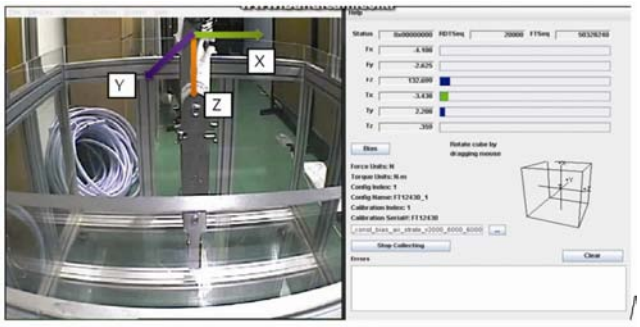

Fig. 9 — Test applying swimming pattern in the air

Numerically buoyancy was very insignificant as much as 10^{-10}N. To verify whether the experimental value is similar, the test as Figure 9 was conducted. (a) is sensor measuring in air and (b) is sensor measuring in water. According to the measuring result, the value was changed very little. That is,

buoyancy needs not to be considered for the robot in operation now.

Drag measuring applying swimming pattern

In this chapter, the pattern in Figure 7 was applied to the robot for the test and the result was recorded. The data from the sensor while robot was moving the legs in the air and water was analyzed.

The left in the Figure 9 shows the test device in the air. No thank was not filled with water. The right is GUI showing the data from the sensor. The output unit is N and NM.

Figure 10 shows the result value from the sensor when testing in the air. Except T_y and F_x, other values were almost 0. Because of moving at uniform velocity, others except T_y which has effect by gravity shall be 0, which indicated the data were correct. The values significant increased in the middle of F_x data was due to the precision degree of the design of robot's each joint.

The left of figure 11 shows the test device in the water. Unlike figure 9, the tank was filled with the water for the test.

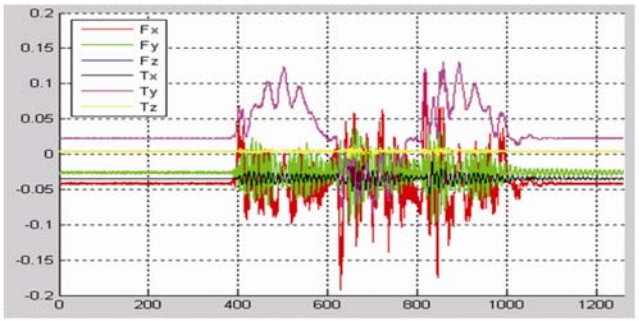

Fig. 10 — Test applying swimming pattern in the air (force/torque sensor data)

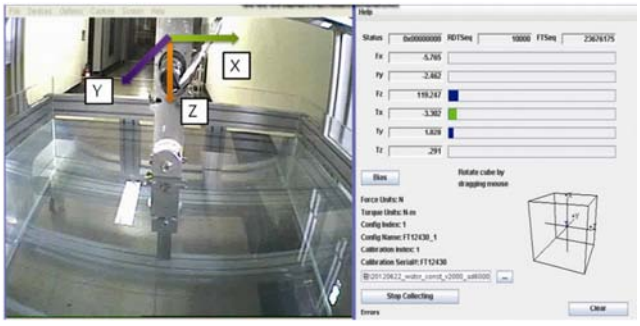

Fig. 11 — Test applying swimming pattern in the water

Figure 12 shows the result value from the sensor when testing in the air. Except T_y and F_x, other values were almost 0. Drag worked in the direction of robot's motion. As the robot moved based on Y axis, F_x was working. Viewing the result from the sensor when testing in the air and the sensor the F_x, the result is as Figure 13.

The data line in red is the test in the air while the data line in blue is the test in the water. As seen from the result, the data from the test in the air was mostly close to 0, while the data from the test in the water indicated the certain pattern depending on motion of the robot.

Figure 14 shows the comparison between the data from the sensor in the water in Figure 13 and the drag data from the simulation. The simulation on top in the left describes the swimming pattern of the robot. The figure on top in center is the drag data from the simulation. The figure at the bottom in the right is the actual drag data obtained by applying the swimming pattern from the simulation. As indicated by the arrow, drag data from the simulation and test data were commonly in a certain pattern depending on robot in motion.

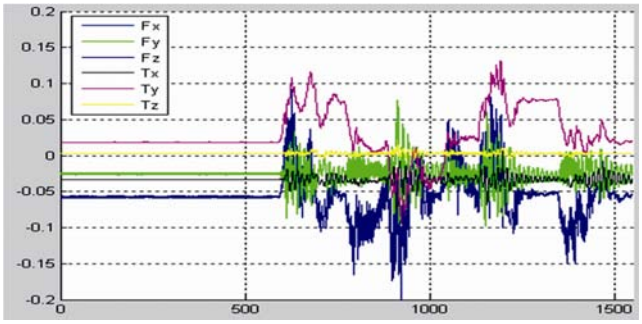

Fig. 12 — Test applying swimming pattern in the water (force/torque sensor data)

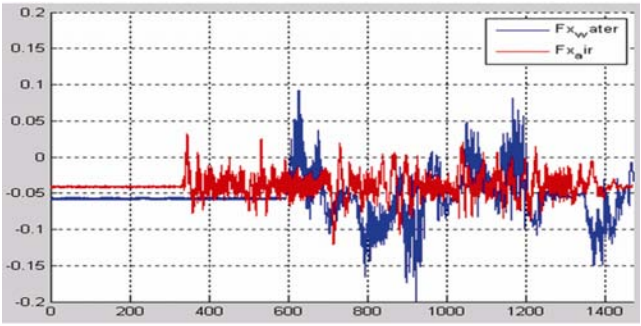

Fig. 13 — Comparison of drag between air and water

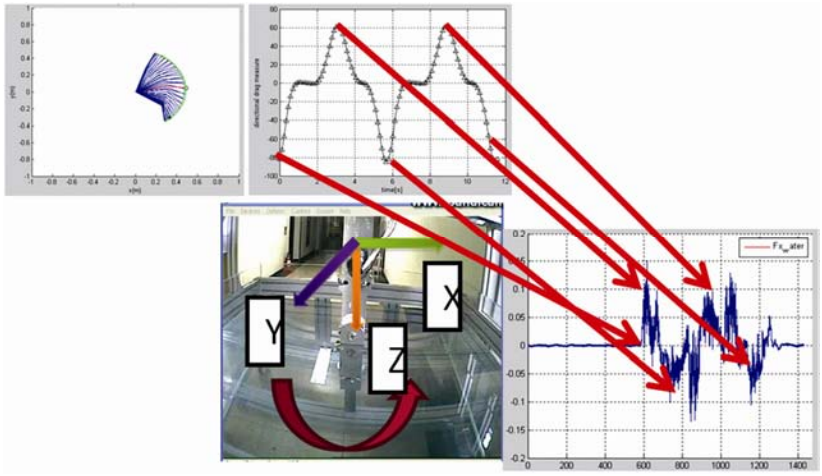

Fig. 14 — Comparison between the drag from simulation and the test

Conclusion

In this study, the drag was measured by applying the swimming pattern of the robot from the simulation to the robot. Moreover, the drag from the simulation and the test was compared and analyzed to apply the data to robot manufacture process. As indicated in 4.2, the drag data from the simulation and the test has a certain pattern in common.

The study will continue in a way of providing the robot with two legs and the simulation will accordingly accommodate two legs, and the study will focus on analysis method as well. Because when swimming with two legs, pumping effect to increase the propelling power is expected, not to mention the propelling power from each leg.

Acknowledgments

This work was supported by the Korea Institute of Ocean Science and Technology (KIOST) and the object is “Development of multi-legged walking and flying subsea robot”.

References

1 Kim Seng-ki. 1999. Nothing new under the Sun – Biomimetics. Health world, v.46, no.8, pp.46-49

2 Park Hoon-cheol, Lee Soon-ki. 2005. Principle of bird/insect’s flapping for study on bird/insect-imitating flying robot, KSAS, v.33, no.6, pp.100-107.

3 Kang Rae-hyung, Chang Hee-sook, Lim Ju-hyung, Han Jae-heung.2009. Manufacture of composite hinge mechanism for micro flapping flying motion. Korean Society for composite materials journal v.22, no.6, pp.7-12.

4 Oh, Sang-jin, Lee jee-hong, Choi Hoon. 2007. Design and modeling of Omni-trade shaped snake robot (CALEB III).2007 Military robot workshop, pp.55-59.

5 Ko Kwang-jin, Yoo Seung-nam, Han Chang-soo. 2007. Test of sensor-based walking of 4-legged biomimetics walking robot.Korean Society for Precision Engineering, 2007 Spring Forum Papers, pp.101-102.

6 Yeo Tae-gyung, Hong Seob, Chun Bong-hwan. 2010. Current trend of the study on underwater multi robot. ICROS, v.16, no.1, pp.23-34.

7 Kim Hyung-seok, Vo Tuong Quan, Lee Byung-ryong, Yoo Ho-young.2009. The study on dynamic analysis of 3-free fish robot and optimization of swimming parameter. Korean Society of Mechanical Engineer papers Book A Vol 33, No 10, pp.1029-1037.

8 Chung Chang-hyun, Lee Sang-hyo, Kim Kyung-sik, Cha Yoo-sung, Ryu Young-seon.2010. Optimization of input parameter using DOE for dynamic analysis of Biomimetics fish robot Ichthus.Journal of Institute of Control, Robotics and Systems vol 16, No 8, pp.799-803.

9 Chun Bong-hwan .Modeling and Drag-Optimized Joint Motion Planning of Underwater Robotic Arms.Ph.D.thesis, Dept. of Mechatronics, Chungnam National Univ. 2006

10 Kim Dae-hyun, Lee Ji-hong, Kim Seok-yong, Lee Jong-hwa, Chun Bong-hwan. 2011. The study on optimal swimming pattern of underwater robot.ICS'11, April, pp.171-172.